

# Thermal driven domain and cargo transport in lipid membranes

Emma L. Talbot, \* Lucia Parolini, \* Jurij Kotar, \* Lorenzo Di Michele, \* and Pietro Cicuta \*

\*Department of Physics, Cavendish Laboratory, University of Cambridge, JJ Thomson Avenue, Cambridge, CB3 0HE, United Kingdom

Submitted to Proceedings of the National Academy of Sciences of the United States of America

**Domain migration is observed on the surface of ternary giant unilamellar vesicles held in a temperature gradient, in conditions where they exhibit coexistence of two liquid phases. The migration localises domains to the hot side of the vesicle, regardless of whether the domain is composed of the more ordered or disordered phase, and regardless of the proximity to chamber boundaries. The spacing of domains is explored for domains which coarsen, and for those held apart due to long range repulsions. After considering several potential mechanisms for the migration, including the temperature preferences for each lipid, the favoured curvature for each phase, and the thermophoretic flow around the vesicle, we show that observations are consistent with the general process of minimising the system's line tension energy, due to the lowering of line interface energy closer to mixing. DNA strands, attached to the lipid bilayer with cholesterol anchors, act as an exemplar "cargo" demonstrating that the directed motion of domains towards higher temperatures provides a route to relocate species that preferentially reside in the domains.**

vesicle | thermal migration | lipid domains | DNA

**G**iant unilamellar vesicles (GUVs) provide a simplified model for studying various aspects of biological membranes. GUVs of a saturated lipid, an unsaturated lipid, and a sterol can form domains of coexisting liquid phases below a critical transition temperature,  $T_t$ . Domains diffuse on the surface of the vesicle with a diffusion coefficient that depends on the domain size and the membrane viscosity [1]. The domain morphology is strongly linked to the temperature and composition of the membrane [2, 3, 4] and also the membrane tension [5]. GUVs have been observed to form a range of shapes [6, 7, 8, 9] and domain morphologies [2, 10], including modulated phases [11]. However, to minimise their edge length, liquid phase domains most commonly form circular patches, and coarsen to reduce the overall line energy over the membrane. "Normal" coarsening can occur by collision and coalescence of domains due to their diffusive motion [12, 13], or by Ostwald ripening [14]. In practice, membrane curvature adds other degrees of freedom, and provides another route to minimise the free energy via domain budding [15, 16, 17]. Domains of the phase with a lower bending modulus may dimple from the surface of the vesicle. Repulsive interactions (associated with curvature of the membrane between domains) keep dimpled domains apart and cause a reduction in the rate of coalescence ("hindered" coarsening) [13, 18].

The behaviour of domains in liquid-ordered ( $L_o$ )/liquid-disordered ( $L_d$ ) phase coexistence has been explored in equilibrium, and during coarsening [12]. Such studies include the fluctuations in the domain boundary observed near  $T_t$  [19], and the dependence of  $T_t$  on the membrane composition [4]. However, these studies look only at a fixed temperature across a domain. While osmotic gradients have been explored to induce shape changes in vesicles [9], temperature gradients have received little attention.

In this paper, we observe the behaviour of domains in a thermal gradient to visualise the effect on transport processes. Domains migrate towards the hot side of a GUV for both "normal" and "hindered" coarsening regimes, regardless of their

phase ( $L_d$  or  $L_o$ ). The lateral transport of domains along a membrane provides a route for tailoring the membrane composition by delivery/removal of the lipids forming these domains. Similarly, species that preferentially locate within the domains (for example, some integral membrane proteins prefer to reside in cholesterol-rich regions [20]) can be moved selectively to heated regions. We use the transport of DNA-constructs with cholesterol anchors, which preferentially locate in the cholesterol-rich  $L_o$  phase [21], to demonstrate this thermal manipulation mechanism.

## Results and Discussion

**Domain migration on the surface of a vesicle.** To explore the migration of domains on the surface of a vesicle we used fluorescence microscopy to image GUVs composed of DiPhyPC/DPPC/cholesterol. The inclusion of a fluorescent lipid (which partitions preferentially into the  $L_d$  phase) allows us to distinguish between bright domains rich in DiPhyPC and dark domains rich in cholesterol and DPPC. A custom-made imaging cell is used to produce a temperature gradient across a GUV. The temperature is first increased above the transition temperature,  $T_t$ , and held for 5 min to ensure that the lipids are fully mixed. The temperature is then quenched below  $T_t$  and domain formation and migration is observed with (or without) a temperature gradient  $\Delta T_v$  across the vesicle. A small density mismatch between an inner solution of sucrose and outer solution of glucose is set, to cause vesicles to sink to the cold plate and facilitate imaging. Following quenching

### Significance

**Giant phospholipid and sterol vesicles can separate into coexisting phase domains, observable by fluorescence microscopy. The morphology and motility of these domains provides a simplified model for processes in the plasma membrane of cells. Previous studies maintained a uniform temperature across a vesicle and showed that the morphology of the domains depends on the membrane composition and temperature. We observe the non-equilibrium behaviour of domains due to a temperature gradient, revealing domain migration towards higher temperatures. This provides a method for controlling the localisation of each phase. Species which associate with the sterol-rich regions, such as DNA-constructs, can also be actively transported on the vesicle surface, allowing control over the distribution and confinement of that species via the vesicle morphology.**

### Reserved for Publication Footnotes

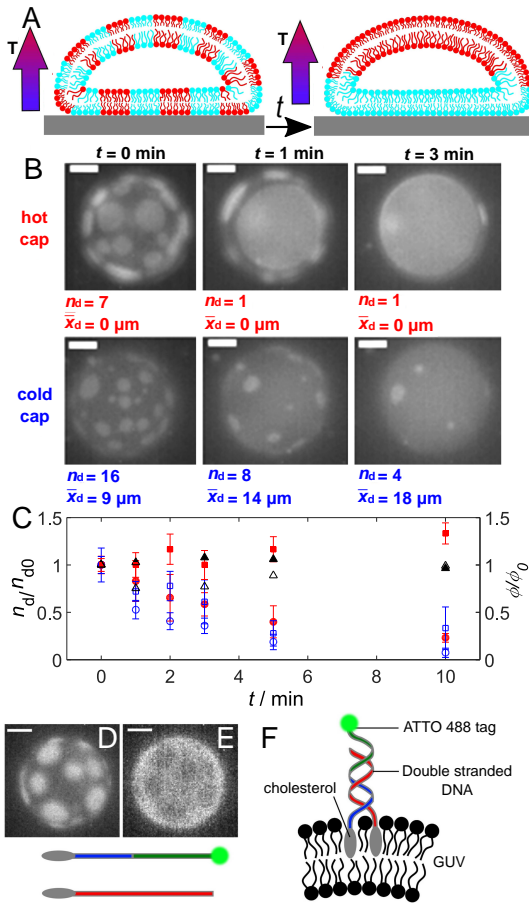


**Fig. 1. Lipid domains migrate to the hot cap of a GUV in a temperature gradient, and can carry associated cholesterol-anchored DNA-constructs.** A) Schematic side-view of the process of domain migration and coalescence. Coalescence increases the size of domains crowded on the hot cap, to form one large domain, aligned with the temperature gradient. B) Migration affects domains over all the GUV; shown here are the hot and cold caps of the same GUV at three time points (all scale bars  $10\ \mu\text{m}$ ).  $\Delta T_V = 2.1\ \text{K}$  across the vesicle. The domain number,  $n_d$ , and mean separation of nearest neighbours (centre-to-centre),  $\bar{x}_d$ , are shown for each cap. C) Mean  $n_d$  ( $\circ$ ), normalised by initial domain number,  $n_{d0}$ , and area fraction of white  $L_d$  domains to vesicle area,  $\phi$  ( $\square$ ), normalised by the initial fraction  $\phi_0$  with respect to time for the cold (open, blue) and hot caps (closed, red). Data are in excess of 50 vesicles. Error bars are standard errors on the mean. For comparison, ( $\triangle$ , closed for the hot side and open for the cold side) are the area fractions of  $L_d$  domains for a vesicle with  $\Delta T = 0$ . Images show (D) TX-DHPE partitioning into the  $L_d$  phase (the circular domains, in this case), and (E) DNA-rich  $L_o$  regions. F) Schematic of DNA-construct anchored to the bilayer. Constructs are assembled from three single stranded sequences (indicated by red, green and blue).

of the sample from above the transition temperature, domains form on the surface of a vesicle. If no temperature gradient is applied the domains coalesce over time, to form a phase separated vesicle with one bright side ( $L_d$ ) and one dark side ( $L_o$ ). The orientation of the  $L_d$  and  $L_o$  phases with respect to the vertical direction is random.

When a vertical temperature gradient is applied across the vesicle, the domains migrate from the cold side around to the hot cap (Fig. 1A). Figure 1B shows an example of the  $L_d$  phase forming the domains. Crowding of the domains on the hot cap results in larger domains due to coalescence, which usually eventually merge to form one large domain on the hot side (the migration also occurs in some vesicles where the coarsening is “hindered” due to curvature mediated domain

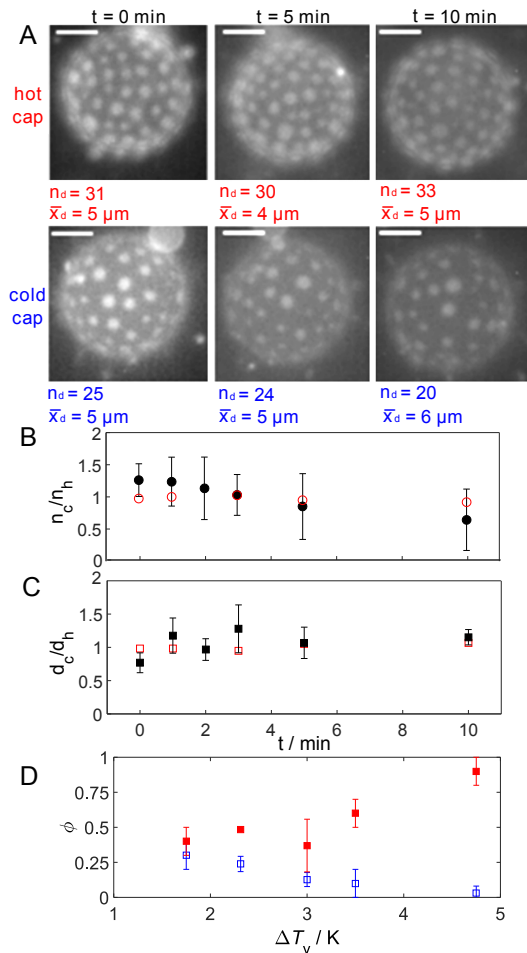


**Fig. 2. Domain spacing can be controlled on a GUV with “hindered” coarsening.** Here, membrane mediated long range repulsions greatly reduce the coalescence rate. Migration increases the number of domains,  $n_d$ , on the hot cap relative to the cold, and increases the mean separation of nearest neighbour domains (centre-to-centre),  $\bar{x}_d$ , on the cold cap. A) Domains on the hot and cold caps of the same GUV with time (scale bars  $10\ \mu\text{m}$ ).  $\Delta T_V = 1.4\ \text{K}$ . B) Mean number of domains on the cold side,  $n_c$ , normalised by the number on the hot side,  $n_h$ , with time (closed). C) Mean domain spacing on the cold side,  $d_c$ , normalised by the spacing on the hot side,  $d_h$  ( $\blacksquare$ ). Data are in excess of 10 vesicles. Also shown, an example vesicle with  $\Delta T = 0$  ( $\square$ ). Error bars are standard errors on the mean. D) Mean area fraction of white domains ( $\blacksquare$  at hot;  $\square$  at cold), relative to total vesicle area, 10 min after initialisation of the temperature gradient.

repulsion [22, 23]). The cold side is thus in all cases depleted of domains. Figure 1C demonstrates quantitatively the increase in the area fraction of white domains ( $A_w/A_v$ ) on the hot cap, and depletion on the cold cap, due to domain migration. The number of domains on the cold cap decreases due to the migration; there is also a decrease on the hot cap, due to coalescence forming fewer larger domains. The domain migration aligns the  $L_d$  and  $L_o$  phases in the fully separated vesicle with the temperature gradient (i.e with the  $z$  direction). Note that if  $T_h \geq T_t$ , domains “disappear” as they enter the one phase region ( $T_t \simeq 38^\circ\text{C}$  for DiPhyPC/DPPC/chol in the ratio 27.5:27.5:45 mol% [4]). In contrast,  $A_w/A_v$  remains constant for a vesicle with  $\Delta T = 0$ , as domains coalesce at a similar rate on each cap and do not migrate.

The crowding of domains is easier to observe in vesicles with “hindered” domains (Fig. 2A), as the coalescence rate is significantly reduced [13]. Figures 2B/C show the closer packing

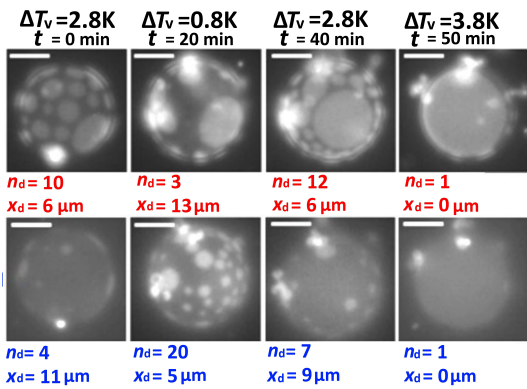


**Fig. 3. Domain migration on a GUV with “hindered” domains is reversible.** For larger  $\Delta T_V$ , domains are depleted from the cold cap. Once  $\Delta T_V$  is decreased, domains move back onto the cold cap ( $t=20\text{ min}$ ). The cold plate was held at  $285\text{ K}$  and  $\Delta T_V$  decreased then increased. Reapplying the temperature gradient returns domains to a crowded state on the hot cap ( $t=40\text{ min}$ ). For  $\Delta T=3.8\text{ K}$ , the barrier to coalescence was exceeded ( $t=50\text{ min}$ ). Scale bars are  $10\ \mu\text{m}$ . The number of domains,  $n_d$ , and the mean separation of nearest neighbour domains (centre-to-centre),  $\bar{x}_d$ , are indicated for each cap of the same GUV.

of domains on the hot cap, while domains on the cold side are more spread out and are relatively fewer in number. The migration is enhanced when a larger temperature difference is applied across the vesicle, which results in an increase in the area fraction of the  $L_d$  phase (which forms the circular domains in this case) on the hot side, and a decrease on the cold side at larger  $\Delta T$  (see Fig. 2D). The “hindered” coarsening also shows that the migration is not linked to differences in coalescence or coalescence rates on the hot cap compared to the cold cap.

The crowding of domains in the “hindered” case is reversible (Fig. 3). Reducing the temperature gradient (or removing it altogether) allows the domains that were previously crowded onto the hot side to migrate back to the cold side (Fig. 3,  $t = 20\text{ min}$ ). Reapplying the temperature gradient returns do-

main to a more clustered arrangement on the hot side of the vesicle (Fig. 3,  $t = 40\text{ min}$ ). However, at large  $\Delta T_V$ , the barrier to coalescence is exceeded (Fig. 3,  $t = 50\text{ min}$ ).

**Migration of species carried within domains.** In this section, we explore the potential for relocating a species associated with the domains of a ternary GUV. DNA-constructs with two cholesterol anchors are one such species, and preferentially associate with the cholesterol-rich  $L_o$  phase domains of a vesicle [21] (Fig. 1D/E). The cholesterol-anchors partition into the membrane (Fig. 1F), and the attached DNA is mobile across the surface of the vesicle (along with its anchor). The degree of partitioning of the DNA-constructs depends on the cholesterol content of each phase and is therefore linked to both the vesicle composition and the temperature.

By combining the migration of domains in a temperature gradient with the association of DNA-constructs with those domains, we show that the DNA-constructs can be redistributed on the surface of the vesicle. If the circular domains are formed from the cholesterol-rich  $L_o$  phase, then the DNA-constructs associate with the domains and migrate toward the hot cap of the GUV (Fig. 4 (left)). However, if the composition of the vesicle is such that the circular domains are formed from the cholesterol-poor  $L_d$  phase, then the majority of DNA-constructs are left behind on the cold side of the vesicle as the  $L_d$  domains migrate to the hot cap (Fig. 4 (right)). Hence, by tailoring the composition of the vesicle, the species associated with the  $L_o$  phase can be directed towards high or low temperatures along a thermal gradient. DNA-constructs have the added potential for modification and/or attachment.

**Domain migration mechanisms.** In this section, we discuss potential mechanisms for the migration. The first possible mechanism is if one lipid has a preference for the hot side over the other lipid, then that lipid would migrate toward higher temperatures. We have already noted that domains formed from the  $L_d$  phase (i.e. predominantly DiPhyPC) migrate toward the hot cap (e.g. Fig. 1). To determine whether there is a

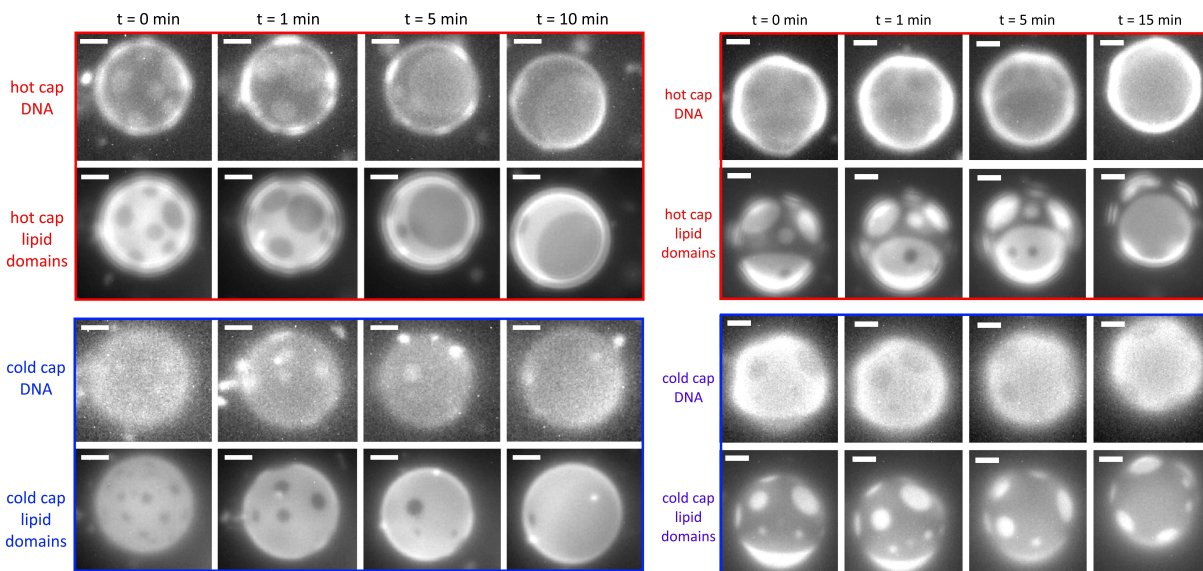


**Fig. 4. Domains and DNA-constructs are co-localised and transported in the temperature gradient.** Images show hot and cold caps of the same GUV (left: DiPhyPC/DPPC/chol 23:47:30 mol%, right: DiPhyPC/DPPC/chol 1:1:1 mol%). DNA-constructs partition preferentially into the  $L_o$  phase. Left:  $L_o$  circular domains migrate towards higher temperatures, depleting the cold cap and leaving it rich in the  $L_d$  phase. DNA-constructs are transported with the  $L_o$  domains to enrich the hot cap of the GUV. Right: DNA “cargo” is left behind on the cold cap as  $L_d$  domains migrate to the hot cap. Scale bars are  $10\ \mu\text{m}$ ,  $\Delta T_V = 2.3\text{ K}$  (left) and  $2.6\text{ K}$  (right).

preference of DiPhyPC for the hot side, we observe domain migration on a vesicle where the domains are instead composed of the  $L_o$  phase (i.e. predominantly DPPC). Figure 5 shows that the  $L_o$  domains also migrate to the hot side, indicating that there is no thermal preference for one lipid over the other. Domains always migrate toward the higher temperature *independent of their composition*.

The second potential migration mechanism is the preference of one of the phases for regions of higher/lower curvature. The mismatch in the density of the sugar solutions inside and outside of the vesicle causes the vesicle to rest on the lower (cold) plate. The solid surface causes deformation, resulting in a curvature difference between the hot and cold sides of the vesicle (as illustrated in the Fig. 1A schematic). Previously,  $L_d$  domains have shown a preference for regions of higher curvature [24]. For GUVs resting on the lower cold plate,  $L_d$  domain migration was toward the hotter side which had a higher curvature as it was not compressed flat by the substrate. To ensure the migration was to regions of higher temperature and not higher curvature, the density mismatch of the sugar solution inside and outside of the vesicle was reversed: GUVs now rise to the hot plate and are compressed on their hot side. Domain migration remained in the direction of the higher temperature and hence migration was *independent of the vesicle curvature, or other terms of affinity for the imaging chamber window*.

The third potential mechanism is the difference in the line tension across a domain due to the temperature gradient across the vesicle. Migration towards hotter temperatures provides a route to minimise the line interface energy of the domains. The line tension,  $\lambda$ , of DiPhyPC/DPPC/chol vesicles decreases linearly over a range of at least  $10^\circ\text{C}$  with increasing temperature close to  $T_i$  [19] and hence  $\Delta\lambda$  across the domain does not depend on the absolute temperature. There is however an effective force due to translating the domain interface towards higher temperature (closer to mixing) since this lowers the line interface energy,  $E$ . The force due to translating a domain of radius  $r$  along the thermal gradient in the  $z$  direction is

$$F_t = \frac{\partial E}{\partial z} = \frac{2\pi r \partial \lambda}{\partial z}. \quad [1]$$

This force is resisted by the drag force,  $F$ , and results in a drift velocity

$$v = \frac{F}{\zeta}, \quad [2]$$

where  $\zeta$  is the drag coefficient, in general related to the diffusion coefficient of a domain,  $D$ , by

$$\zeta = \frac{k_B T}{D}, \quad [3]$$

where  $k_B$  is the Boltzmann constant and  $T$  is the absolute temperature.

The form of the drag coefficient is dependent on the domain size [25, 1]. For small domains ( $r < \eta''/\eta_w$ ), the drag coefficient has the Saffman-Delbruck form and is also dependent on the membrane viscosity:

$$\zeta(r) = \frac{4\pi\eta''}{\left[\ln\left(\frac{\eta''}{\eta_w} \frac{1}{r}\right) - \gamma + \frac{1}{2}\right]}, \quad [4]$$

where  $\eta''$  is the 2D membrane viscosity ( $\simeq 10^{-8} \text{ N s m}^{-1}$  [1]),  $\eta_w$  is the 3D bulk viscosity (of water,  $\simeq 10^{-3} \text{ Pa s}$ ), and  $\gamma (=0.5772)$  is Euler's constant. For larger domains ( $r > \eta''/\eta_w$ , approximately  $r > 10 \mu\text{m}$  in this case), the drag coefficient is independent of the membrane viscosity,

$$\zeta(r) = 16\eta_w r. \quad [5]$$

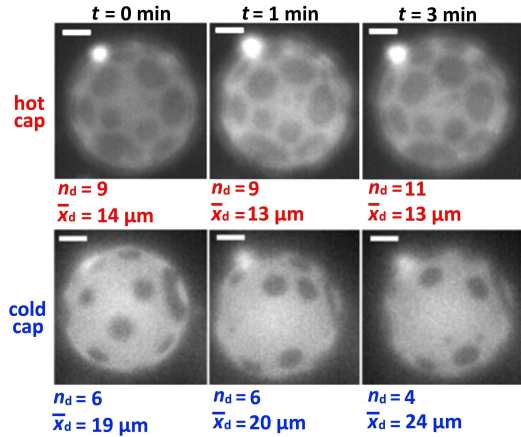


**Fig. 5. Domain migration to the hot cap is independent of lipid species.** Circular domains of the  $L_o$  phase also migrate towards the hot cap, indicating there is no preference of one lipid over the other for the hot side. Domains in a GUV with “hindered” coarsening are shown on the hot and cold caps; time is measured from the quench below  $T_i$  ( $\Delta T_v = 1.4 \text{ K}$ ). Scale bars are  $10 \mu\text{m}$ . The number of domains,  $n_d$ , increases on the hot cap, and the mean centre-to-centre distance of nearest neighbour domains,  $\bar{x}_d$ , decreases relative to the cold cap.

In our case, we consider only domains with  $r < 10 \mu\text{m}$ , and therefore use equation 4 for our calculations.

Let us estimate the drift velocity of a domain of  $5 \mu\text{m}$  diameter. The temperature gradient is  $\partial T/\partial z = 1/10 \text{ K}/\mu\text{m}$ . The change in line tension with temperature is  $d\lambda/dT = 0.1 \text{ pN K}^{-1}$ . Thus considering the domain perimeter, following the argument above, the force is  $0.15 \text{ pN}$ . The drag coefficient of domains on the cold side of a  $30 \mu\text{m}$  diameter GUV ( $T = 299 \text{ K}$ ,  $\Delta T_v \simeq 3 \text{ K}$ ) can thus be estimated  $\zeta \simeq 9 \times 10^{-8} \text{ N s m}^{-1}$  for domains with a radius of  $2.5 \mu\text{m}$  using eq. 4. Therefore the corresponding drift velocity (from eq. 2) is  $1.5 \mu\text{m s}^{-1}$ . This number can be compared to the experimentally observed drift, keeping in mind that this estimate is only expected to hold as an order of magnitude because of (a) the uncertainty on the precise value of membrane viscosity (and its change across the vesicle) and (b) the fact that we do not observe domain displacements purely along the temperature gradient axis. Tracking domains of mean radius  $r \simeq 2.5 \mu\text{m}$  on the surface of a  $30 \mu\text{m}$  GUV provides a measure of the domain drift velocity of  $v \simeq 0.4 \mu\text{m s}^{-1}$  for  $\Delta T_v \simeq 3 \text{ K}$ . Approximately 20 domains were tracked on the vesicle surface. This is of the same order as what we estimated from the line tension argument, and suggests that this is indeed the mechanism for the migration of domains toward the hot cap of a vesicle. A further corroboration comes from comparing measurements of the mean squared displacement of domains with/without an applied temperature gradient. When no thermal gradient is applied, domains follow diffusive motion (Fig. 6). However, on applying a thermal gradient, domains begin to move with a drift velocity (dependent on the domain radius and temperature) towards the hot side of the GUV. This drift velocity is predicted well by the line tension mechanism using equations 1–4 (Fig. 6B).

The membrane viscosity has a strong temperature dependence, decreasing at higher temperatures [1], which would in turn progressively lower the drag coefficient (thus increase the mean squared displacement) of domains migrating to the hot side. This could contribute to a higher than linear dependence of the msd on time, as the domain moves to hot, but does not seem to us sufficient to explain the driven migration, and neither the magnitude of the observed msd: for a domain radius  $= 1.25 \mu\text{m}$ , with a temperature on the cold

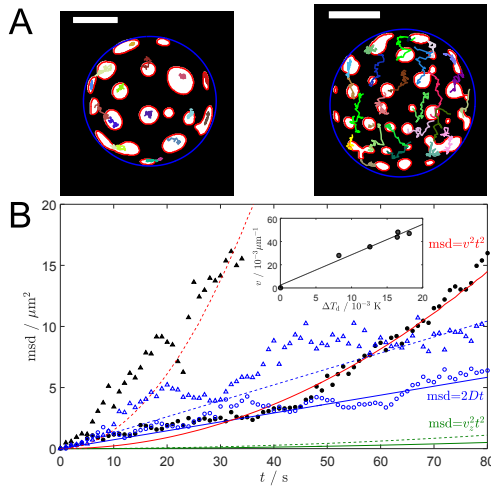


**Fig. 6. Domains drift in a thermal gradient towards the hot cap, and follow diffusive motion for  $\Delta T = 0$ .** A) Domain tracks for a typical GUV (temperature cold side,  $T_c = 288\text{ K}$ ) with  $\Delta T = 0$  (diffusive motion only) and  $\Delta T = 15\text{ K}$  (combined diffusive and directed motion) over a 40 s period, superposed to initial positions of domains (segmented, in white) on the cold side of a GUV (diameter  $\sim 30\ \mu\text{m}$ ). The blue circle indicates the GUV perimeter and red lines show domain boundaries. B) Mean squared displacement (msd) for  $\Delta T = 0$  (blue data, solid fits) and  $\Delta T = 15\text{ K}$  (black data, dashed fits) at  $T_c = 288\text{ K}$  (o) and  $T_c = 299\text{ K}$  ( $\Delta$ ). Fits show msd assuming diffusive motion with: the Saffman-Delbruck form of the drag coefficient (blue); thermal drift driven by the variation in line tension across a domain (red); and a thermophoretic mechanism (green). Insert shows the linearity of drift velocity,  $v$ , against temperature difference across a domain,  $\Delta T_d$  (mean domain radius  $1.25\ \mu\text{m}$  and mean GUV radius  $14\ \mu\text{m}$ ).

cap of 288K and on the hot cap of 291K, membrane viscosity  $\simeq 2 \times 10^{-8}\ \text{N s m}^{-1}$  at 291 K, then based on diffusion the  $\text{msd}(80\text{s}) \simeq 6.72\ \mu\text{m}^2$ . This  $\text{msd}(80\text{s})$  is far lower than the observed  $\text{msd}$  in the thermal gradient ( $\simeq 15\ \mu\text{m}^2$ ) which we attribute to thermal drift.

It is worth noting that the variation in line tension with temperature is dependent on the chain length of the saturated lipid. In addition, the chain length of the saturated lipid also influences the membrane viscosity. For small domain sizes ( $r < \eta''/\eta_w$ ), the drag coefficient is dependent on the membrane viscosity and as such the chain length of the lipid will also influence the drift velocity in this manner.

An additional mechanism to consider is that the temperature-dependent interactions between the GUV and the surrounding solvent could generate a thermophoretic flow field around the vesicle [26]. For a thermophobic vesicle, the flow across the surface of the vesicle is toward the hot cap. We explore whether the magnitude of this flow is significant enough to drag domains on the surface of the vesicle towards the hot side (Note that a thermal Marangoni flow in the membrane would be directed towards colder regions, where the surface tension would be higher, and as such is not a viable mechanism for domain migration to the hot cap). For large particles, the thermophoretic force can be approximated as in [26], by

$$F_T = -S_T T k_B \nabla T, \quad [6]$$

where  $S_T$  is the Soret coefficient. In response to the thermophoretic force, an equal opposite reaction in the surrounding solvent generates a flow around the surface of the vesicle. Balancing  $F_T$  against Stokes' drag allows an estimate of the velocity in the  $z$ -direction to be calculated, from

$$v_z = -\frac{S_T T k_B \nabla T}{6\pi\eta_w a}, \quad [7]$$

where  $a$  is the radius of the vesicle.

A proportional relationship has previously been established between the radius of a particle,  $a$ , and the magnitude of the Soret coefficient,  $S_T$ , for polystyrene beads [27]. Based on this relationship, a polystyrene bead with  $a = 15\ \mu\text{m}$ , has  $S_T \simeq 90\ \text{K}^{-1}$ . We have found the Soret coefficients of  $1\ \mu\text{m}$  vesicles to be an order of magnitude less than polystyrene particles of the same size and therefore use an upper estimate of the Soret coefficient for vesicles ( $a = 15\ \mu\text{m}$ ) of  $9\ \text{K}^{-1}$ . For a temperature gradient of  $0.1\ \text{K}\ \mu\text{m}^{-1}$ , an upper estimate of the velocity on the cold side of the vesicle ( $T = 299\text{ K}$ ) is  $v_z \simeq 0.01\ \mu\text{m s}^{-1}$ , which corresponds to a thermophoretic force of  $F_T \simeq 4 \times 10^{-3}\ \text{pN}$ . This velocity is much smaller than the observed drift velocity of the domains (Fig. 6B). Furthermore, the drift velocity varies linearly with the temperature difference across a domain.

Lastly, an observation: the non-interface ('bulk') parts of the vesicle membrane coexist at different temperatures. To get a sense of what this implies requires thinking of a specific model for the bulk free energy (e.g a regular solution theory for a binary mixture). If one thinks of a "regular solution" binary mixture and assumes the enthalpic term to be athermal, then it can be shown that the bulk free energies are temperature dependent. However, for each "parcel" of membrane of one phase that migrates from hot to cold, there is one of the other phase that goes the other way. Each of these parcels equilibrates concentrations (following temperature equilibration) with its new surroundings. So for a perfectly symmetric free energy functional, like the one of a regular binary mixture, the changes in bulk free energy of the two parcels will exactly cancel out in the swap, and the net bulk free energy change would be zero. If the bulk free energy functional were substantially asymmetric, then one specific phase would prefer the hot, and the other the cold. However, this is not compatible with the experimental observation that the small domains are systematically driven towards the hot, regardless of their phase.

## Conclusion

When a temperature gradient is applied across a GUV, domains migrate across the surface of the vesicle towards higher temperatures. Migration occurs independent of whether the domains are formed predominantly from the liquid-ordered or the liquid-disordered phase. For vesicles which experience "normal" coarsening, the domains migrate towards the side of the vesicle at a higher temperature due to the mismatch in line tension across a domain. By moving towards hotter temperatures, the domains minimise their line interface energy. The domains also coalesce, resulting in a phase separated vesicle with a single liquid-ordered domain and a single liquid-disordered domain aligned with the direction of the temperature gradient. For "hindered" coarsening regimes, the domain coalescence rate is slowed. In this case, the domain spacing may be reversibly altered by applying or removing the temperature gradient. Domains on the cold side are further apart than on the hot side when the thermal gradient is applied.

By including a species that preferentially associates with the domains of a ternary GUV, that species can be selectively moved and even localised on the surface of a vesicle. DNA-constructs with cholesterol anchors preferentially locate within the cholesterol-rich  $L_o$  phase. Domain migration relocates the DNA-constructs to the cold side of the vesicle if domains are the  $L_d$  phase. If the  $L_d$  and  $L_o$  phases are switched, then the DNA-constructs (which are now associated with the  $L_o$  domains) instead locate to the hot side of the vesicle. DNA-constructs provide an easy route for modification or attachment of other species, which could then be distributed over

the vesicle. The same principle could be applied to proteins which have a composition preference. Similarly, local heating of a supported bilayer with mobile domains could enable directed motion of species associated with the domains.

## Materials and Methods

**Ternary GUVs.** Vesicles were prepared via electroformation [28, 29] from dipalmitoylphosphatidylcholine (DPPC, chain melting temperature  $41^{\circ}\text{C}$ ), diphytanoylphosphatidylcholine (DiPhyPC, chain melting temperature  $<-120^{\circ}\text{C}$ ), and cholesterol (chol). Lipids were purchased from Avanti Polar Lipids (Alabaster, AL) in chloroform and used in the molar ratio 27.5:27.5:45 (DPPC:DiPhyPC:chol). Cholesterol (Sigma-Aldrich) was used in place of cholesterol to reduce photo-oxidation. A fluorescent lipid labeled with Texas red dye, 1,2-dihexadecanoyl-sn-glycero-3-phosphoethanolamine, triethylammonium salt (TX-DHPE), was purchased from Invitrogen and included at 0.8 mol%. The fluorescent lipid partitions preferentially into the  $L_d$  phase. GUVs were prepared to include an inner solution of 197 mM sucrose (Sigma-Aldrich) and an outer solution of 200 mM glucose (Sigma-Aldrich) to ensure that the vesicles rested on the bottom surface.

**DNA-constructs.** Cholesterol anchors on DNA-constructs provide a hydrophobic modification sufficient to allow spontaneous insertion into the bilayer. Such constructs show a compositional preference when associating with the phase domains of a vesicle. The constructs are self-assembled from the following single stranded DNA sequences: 5-CGTGCCTGGCGTCTGAAAGTCGATTGCGAAAA-3-CholesterolTEG (Integrated DNA technologies), CholesterylTEG-5TTTTTCGAATCGACTTT-3 (Eurogentec), and 5-CAGACGCCAGCGCAGAAA-3 - ATTO488 (Integrated DNA technologies). Single stranded DNA sequences were purchased lyophilised, reconstituted in TE buffer (10 mM tris(hydroxymethyl)aminomethane, 1 mM ethylenediaminetetra acetic acid, Sigma Aldrich), and mixed in stoichiometric ratio in TE buffer with 100 mM NaCl. The mixture is heated to  $90^{\circ}\text{C}$  and cooled slowly to enable the self-assembly of the DNA-construct shown in Fig. 1F. The ATTO488 dye enables fluorescence microscopy of the DNA-constructs. GUVs containing 300 mM sucrose are prepared via electroformation (to ensure vesicles are denser than the surrounding solution) and are functionalised by mixing  $2\ \mu\text{L}$  of the GUV sample with  $90\ \mu\text{L}$  iso-osmolar TE buffer solution containing 87 mM glucose, 100 mM NaCl and DNA-constructs. The final concentration of DNA-constructs is  $0.15\ \mu\text{M}$ . DNA-coated vesicles were left under rotation at room temperature overnight to enable DNA binding. The solution was then removed

from rotation and vesicles were allowed to sink for 5-10 min before a sample of  $30\ \mu\text{L}$  was extracted from the bottom of the vial for use in the experiments. Further details on the DNA preparation and vesicle coating can be found in [30].

**Imaging.** A custom-made imaging cell was prepared consisting of a  $200\ \mu\text{m}$  thick silicone spacer (possessing a hole to contain the vesicle suspension), sandwiched between two sapphire windows. The windows were placed on a cooled metal plate connected to a water bath and held on top by a heated metal plate. A central hole was cut into the plates to enable imaging of the vesicles. Thermocouples were used to measure the temperature of the plates. The temperature of the hot plate,  $T_h$ , was held fixed using a custom-built temperature-controller with a feedback loop. The applied linear temperature gradient ( $\Delta T$ ) was vertical with a hotter upper surface, to avoid convection. For imaging DNA-coated vesicles, Bovine Serum Albumin (BSA, Sigma-Aldrich, rehydrated in water to form a 1% solution) was used to passivate glass cover slips which were "stuck" to the sapphire windows with a little water so the DNA/vesicle suspension was not directly in contact with the sapphire.

Fluorescence imaging of the vesicles was carried out using a Nikon Eclipse Ti-E inverted microscope equipped with a  $40\times$  objective lens (Nikon, S Plan Fluor, ELWD 2.8–3.6 mm, NA 0.6) and a camera (Point Grey Research, Grasshopper3 GS3-U3-23S6M). Samples were illuminated with either a metal halide lamp or a single-colour LED through a Texas Red filter set (Semrock, exciter FF01-562/40, dichroic FF593-Di02, emitter FF01-624/40). A z-stack was taken across the vesicle and the slices were analysed using custom-made MATLAB image analysis routines. The slice showing the domains on the top side is referred to from here on as the hot cap, and the bottom side as the cold cap. For DNA-coated vesicles, the DNA was imaged using a GFP filter set (Semrock, exciter FF01-472/30, dichroic FF495-Di03, emitter FF01-520/35).

**ACKNOWLEDGMENTS.** This work was supported by EPSRC (grant number EP/J017566/1), and LDM was further supported by Oppenheimer Fund, Emmanuel College Cambridge, Leverhulme Trust and Isaac Newton Trust through an Early Career Fellowship. A complete dataset is available for download at <https://doi.org/10.17863/CAM.6589>.

**Author contributions:** ELT carried out the experiments, analysed data and wrote the paper; LP carried out preliminary experiments and protocol development; JK designed and constructed the experimental apparatus; LDM designed the DNA cargo and wrote the paper; PC posed the research question and wrote the paper.

- Cicuta, P, Keller, S, & Veatch, S. (2007) Diffusion of liquid domains in lipid bilayer membranes. *J. Phys. Chem. B Lett.* 111, 3328–3331.
- Veatch, S & Keller, S. (2003) Separation of liquid phases in giant vesicles of ternary mixtures of phospholipids and cholesterol. *Biophys. J.* 85, 3074–3083.
- Veatch, S & Keller, S. (2005) Seeing spots: Complex phase behavior in simple membranes. *Biochim. Biophys. Acta* 1746, 172–185.
- Veatch, S, Gawrisch, K, & Keller, S. (2006) Closed-loop miscibility gap and quantitative tie-lines in ternary membranes containing Diphytanoyl PC. *Biophys. J.* 90, 4428–4436.
- Chen, D & Santore, M. (2014) Large effect of membrane tension on the fluid-solid phase transitions of two-component phosphatidylcholine vesicles. *PNAS* 111, 179–184.
- Baumgart, T, Hess, S, & Webb, W. (2003) Imaging coexisting fluid domains in biomembrane models coupling curvature and line tension. *Nature* 425, 821–824.
- Yu, Y & Granick, S. (2009) Pearling of lipid vesicles induced by nanoparticles. *J. Am. Chem. Soc.* 131, 14158–14159.
- Yoon, Y.-Z, Hale, J, & Petrov, P. (2010) Mechanical properties of ternary lipid membranes near a liquidliquid phase separation boundary. *J. Phys.: Condens. Matter* 22, 062101.
- Tomita, T, Sugawara, T, & Wakamoto, Y. (2011) Multitude of morphological dynamics of giant multilamellar vesicles in regulated nonequilibrium environments. *Langmuir* 27, 10106–10112.
- Gutleider, E, Gruhn, T, & Lipowsky, R. (2009) Polymorphism of vesicles with multi-domain patterns. *Soft Matter* 5, 3303–3311.
- Amazon, J, Goh, S, & Feigensohn, G. (2013) Competition between line tension and curvature stabilizes modulated phase patterns on the surface of giant unilamellar vesicles: A simulation study. *Phys. Rev. E* 87, 022708.
- Stanich, C, Honerkamp-Smith, A, Putzel, G. G, Warth, C, Lamprecht, A, Mandal, P, Mann, E, Hua, T.-A, & Keller, S. (2013) Coarsening dynamics of domains in lipid membranes. *Biophys. J.* 105, 444–454.
- Yanagisawa, M, Imai, M, Masui, T, Komura, S, & Ohta, T. (2007) Growth dynamics of domains in ternary fluid vesicles. *Biophys. J.* 92, 115–125.
- Lifshitz, I & Slyozov, V. (1961) The kinetics of precipitation from supersaturated solid solutions. *J. Phys. Chem. Solids* 19, 35–50.
- Lipowsky, R. (1992) Budding of membranes induced by intramembrane domains. *J. Phys. II France* 2, 1825–1840.
- Lipowsky, R. (1993) Domain-induced budding of fluid membranes. *Biophys. J.* 64, 1133–1138.
- Lipowsky, R & Dimova, R. (2003) Domains in membranes and vesicles. *J. Phys.: Condens. Matter* 15, S31–S45.
- Ursell, T, Klug, W, & Phillips, R. (2009) Morphology and interaction between lipid domains. *PNAS* 106, 13301–13306.
- Honerkamp-Smith, A, Cicuta, P, Collins, M, Veatch, S, den Nijs, M, Schick, M, & Keller, S. (2008) Line tensions, correlation lengths, and critical exponents in lipid membranes near critical points. *Biophys. J.* 95, 236–246.
- Samsonov, A, Mihalov, I, & Cohen, F. (2001) Characterization of cholesterol-sphingomyelin domains and their dynamics in bilayer membranes. *Biophys. J.* 81, 1486–1500.
- Beales, T & Vanderlick, T. (2009) Partitioning of membrane-anchored DNA between coexisting lipid phases. *J. Phys. Chem. B* 113, 13678–13686.
- Semrau, S, Idema, T, Schmidt, T, & Storm, C. (2009) Membrane-mediated interactions measured using membrane domains. *Biophys. J.* 96, 4906–4915.
- Idema, T, Semrau, S, Storm, C, & Schmidt, T. (2010) Membrane mediated sorting. *Phys. Rev. Lett.* 104, 198102.
- Feriani, L, Cristofolini, L, & Cicuta, P. (2015) Soft pinning of liquid domains on topographical hemispherical caps. *Chem. Phys. Lipids* 185, 78–87.
- Saffman, P & Delbrück, M. (1975) Brownian motion in biological membranes. *Proc. Natl. Acad. Sci.* 72, 3111–3113.
- Yang, M & Ripoll, M. (2013) Thermophoretically induced flow field around a colloidal particle. *Soft Matter* 9, 4661–4671.
- Braibanti, M, Vigolo, D, & Piazza, R. (2008) Does thermophoretic mobility depend on particle size? *Phys. Rev. Lett.* 100, 108303.
- Angelova, M & Dimitrov, D. (1989) Liposome electroformation. *Faraday Discuss. Chem. Soc.* 81, 303–311.
- Angelova, M, Soléau, S, Méléard, P, Faucon, J.-F, & Bothorel, P. (1992) Preparation of giant vesicles by external ac fields. kinetics and applications. *Prog. Colloid Polym. Sci.* 89, 127–131.
- Parolini, L, Mognetti, B, Kotar, J, Eiser, E, Cicuta, P, & Michele, L. D. (2015) Volume and porosity thermal regulation in lipid mesophases by coupling mobile ligands to soft membranes. *Nature Comm.* 6, 1–10.